

Immediate-Early Transcription over Covalently Joined Genome Ends of Bovine Herpesvirus 1: the *circ* Gene

CORNEL FRAEFEL, URS V. WIRTH,† BERND VOGT, AND MARTIN SCHWYZER*

*Institute of Virology, Faculty of Veterinary Medicine, University of Zürich,
Winterthurerstrasse 266a, CH-8057 Zürich, Switzerland*

Received 16 September 1992/Accepted 9 December 1992

Herpesvirus genomes are linear molecules in virions. Prior to replication in host cells, they form circular templates by unknown mechanisms. Examining lytic infection with bovine herpesvirus 1, we observed immediate-early transcription over joined genome ends, which suggested that circles are present at the initial stage of infection. Among the transcripts was a spliced immediate-early RNA (1.5 kb) sharing exon 1 with previously described major immediate-early transcripts from the right genome end and exon 2 with a late transcript located near the left genome end. Exon 2 encodes a putative *circ*-encoded protein with homology to the varicella-zoster virus open reading frame 2 and equine herpesvirus 1 open reading frame 3 products. The novel features reported here for bovine herpesvirus 1 may constitute a more general property of herpesviruses.

Bovine herpesvirus 1 (BHV-1), the causative agent of infectious rhinotracheitis and pustular vulvovaginitis, is a major pathogen of cattle and an economic burden to farmers (20). The lytic cycle of infection comprises three distinct temporal phases named immediate-early (IE), early, and late (10). The IE phase, about 0 to 2 h postinoculation (p.i.), does not depend on newly synthesized viral proteins and is initiated even in the presence of inhibitors of translation. The early phase, about 2 to 5 h p.i., depends on viral regulatory IE proteins synthesized in the preceding phase and generates proteins required mainly for nucleic acid metabolism. The late phase, from about 5 h p.i. until complete cell lysis at 10 to 20 h p.i., is devoted to viral DNA replication, synthesis of structural proteins, and assembly of viral particles. In virions, the BHV-1 genome is a linear double-stranded DNA of 138 kb subdivided into a unique long segment, U_L (105 kb); a unique short segment, U_S (11 kb); and inverted internal, IR_S , and terminal, TR_S , repeat sequences (11 kb each) flanking the U_S segment. Within cells, BHV-1 genomes serving as templates for DNA replication are circular molecules (6). Progeny DNA is formed as head-to-tail concatemers which are subsequently cleaved into unit-length BHV-1 DNA (6). In replicative intermediates, therefore, template DNA, as well as progeny DNA, exhibits covalently joined left and right genomic termini (Fig. 1A and B). The mechanisms involved in circularization and concatemer cleavage are poorly understood, and the time course of these processes has not been determined.

During analysis of the three major BHV-1 IE genes, which occupy the inverted repeats and extend into the adjacent right-hand end of U_L (17-19), we discovered additional IE transcripts hybridizing with probes from the left-hand end of U_L . In this study, we characterized these novel transcripts by Northern (RNA) blotting, primer extension, and polymerase chain reaction (PCR) and showed that an unspliced precursor RNA (6.3 kb) and a spliced IE RNA (1.5 kb) arise by transcription over the TR_S - U_L junction of the genomic termini, suggesting that circular genomes are present during

the IE phase, long before onset of DNA replication. Furthermore, sequence analysis showed that the U_L part of the spliced IE transcript is 3' coterminal with an unspliced late transcript (1.1 kb) and that both contain the same open reading frame (ORF) of 247 codons. The predicted protein exhibits homology with the varicella-zoster virus (VZV) ORF2 and equine herpesvirus 1 (EHV-1) ORF3 products and is designated the *circ*-encoded protein because of its possible origin from a circular BHV-1 genome.

MATERIALS AND METHODS

Virus, cell culture, and transcript-mapping procedures.

Virus strains (K22 and Jura), infection of MDBK cell cultures, treatment with metabolic inhibitors, isolation of total RNA, Northern blotting, S1 nuclease protection, and primer extension analysis have been described previously (19).

Plasmids and sequence analysis. Plasmid p182 contains the BHV-1 K22 *Hind*III N fragment from the left genome end (0 to 0.018 map unit [m.u.]), and p151 contains the adjacent *Hind*III J fragment (0.018 to 0.083 m.u.), both cloned into pUC9 (3). Plasmids N1 to N5 are subfragments of p182 (see Fig. 1C), and plasmids C1 (0.9-kb *Asn*I-*Sal*I fragment; 0.738 to 0.747 m.u.), C2, and C3 (Fig. 1C) are subfragments of previously described plasmid pJuC (19), which contains the BHV-1 Jura *Hind*III C fragment (0.733 to 0.852 m.u.). The nucleotide sequences of p182 and part of p151 were determined by the dideoxy method (14) by using double-stranded plasmids as templates for Sequenase (United States Biochemical, Cleveland, Ohio) with 7-deaza-dGTP or dITP instead of dGTP. The plasmids described above and additional subclones generated with *Nar*I, *Hpa*I, and *Xho*I were sequenced from both strands as required. Sequences were analyzed by using University of Wisconsin Genetics Computer Group programs (2).

Primers and PCR. Oligonucleotide o22 (5'-TCTAGTA GAACAGCGTGGCT-3') is complementary to nucleotides (nt) 547 to 527 in the sequence reported below (see Fig. 4B); o10 (5'-GGTACCTCCGCCGCTGCGCGCTTT-3') represents nt 2487 to 2510 (see Fig. 4A) but contains two deliberate mismatches (G instead of T at nt 2487 creates a *Kpn*I site; T at nt 2501 is correct for Jura but reads G for K22; G at nt 2504 is correct for K22 but reads C for Jura); o3 (5'-

* Corresponding author.

† Present address: Junior College KZO, Stägenbuck, CH-8600 Dübendorf, Switzerland.

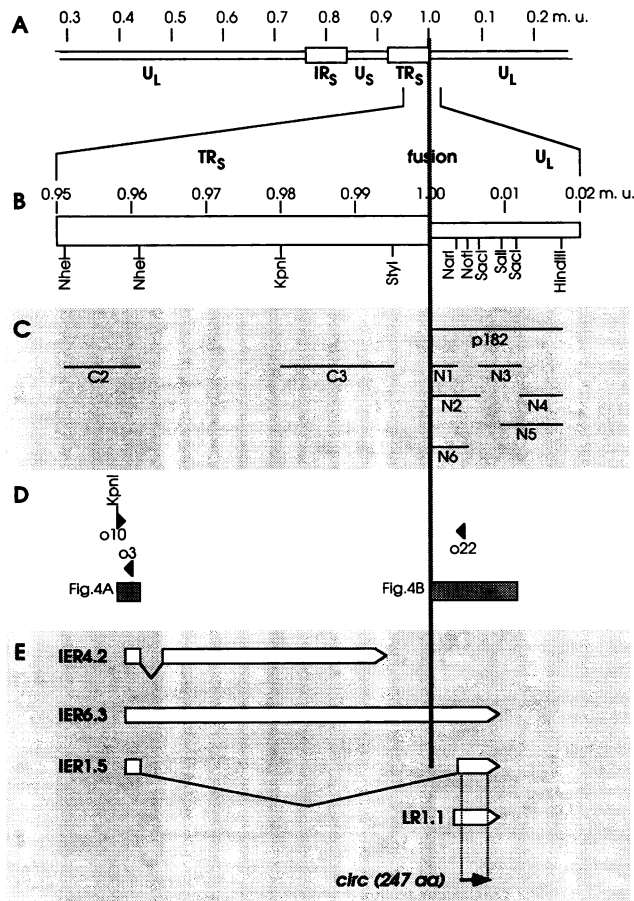


FIG. 1. Map of BHV-1 genome termini. (A) The BHV-1 genome (138 kb) with U_L , U_S , IR_S , and TR_S regions. In accordance with the rest of the figure, the genome is represented with joined termini and an arbitrary interruption in U_L . (B) Covalently joined termini from 0.95 to 1 and 0 to 0.02 m.u. with restriction sites. (C) Locations of probes used for Northern blotting and S1 nuclease analyses. (D) Locations of oligonucleotides used for primer extension and PCR; nucleotide sequences reported here. (E) Transcript map established in this study; ORF for the *circ*-encoded protein. aa, amino acids.

TTGGCCGTCTCCTCCTTCC-3') is complementary to nt 2586 to 2568 (see Fig. 4A); o22 and o10 were used as PCR primers, and o3 (19) was used as a probe (Fig. 1D). Unlabeled o22 was hybridized to RNA (5 μ g) from mock-infected or BHV-1 K22-infected, cycloheximide-treated cells and extended with reverse transcriptase. After phenol extraction and ethanol precipitation, extension products were transferred to PCR mixtures (30 μ l) containing 10 pmol of o10, 10 pmol of o22, 10 mM Tris-HCl (pH 8.3), 50 mM KCl, 1.5 mM $MgCl_2$, 0.2 mM each dNTP, 7.5% dimethyl sulfoxide, and 0.01% gelatin. After initial denaturation at 98°C for 3 min, 1.5 U *Taq* polymerase (Cetus-Perkin Elmer, Küssnacht, Switzerland) was added and PCR was performed for 32 cycles (30 s at 95°C, 1 min at 50°C, 1 min at 72°C) in a Hybaid heating block (AMS Biotechnology, Bioggio, Switzerland). After final extension (10 min at 72°C) and phenol-chloroform extraction, PCR products were analyzed on a 2% agarose gel.

Nucleotide sequence accession number. The nucleotide sequence data for the *circ* gene (this report) and the BHV-1 homolog of the UL54 gene of herpes simplex virus type 1

(HSV-1) (4) have been submitted to GenBank and assigned accession no. M96453.

RESULTS

An unspliced precursor RNA (6.3 kb) and a spliced IE RNA (1.5 kb) arise by transcription over the TR_S - U_L junction of the genomic termini. As a guide to the experiments described below, Fig. 1 shows the map locations of hybridization probes (panel C) and oligonucleotide primers and sequenced regions (panel D) and a summary of the deduced transcript pattern (panel E). Transcripts were first mapped by Northern blot analysis of RNA from BHV-1 strain K22-infected or mock-infected cells (Fig. 2). Cycloheximide was used to block translation in the IE phase and to induce accumulation of IE transcripts. Hybridization with the probe representing the left genome terminus of BHV-1 (p182; *HindIII*-N) revealed two specific IE transcripts, IER6.3 and IER1.5 (Fig. 2A, lane 4). The band around 4 kb comigrated with bulk 28S rRNA, which had been shown earlier to cause nonspecific cross-hybridization (18), and was therefore not interpreted as a specific IE transcript. In accordance with previous results (19), probe pJuC (*HindIII*-C; 0.733 to 0.852 m.u.), containing the entire inverted repeat of BHV-1 with the adjacent U_L and U_S segments, revealed the major IE RNAs (IER4.2, IER2.9, and IER1.7), a 7-kb unspliced precursor of IER2.9, and a less abundant transcript shown below to be identical to IER6.3 (Fig. 2A, lane 2). Transcripts harvested at different times p.i. in the absence of cycloheximide and probed with p182 (Fig. 2A, lanes 6 to 9) exhibited an early RNA (IER1.7) that appeared at 3 h p.i., followed by two late species (LR1.1 and LR3.0), confirming earlier results (18). Under these conditions, IER6.3 and IER1.5 remained below the limit of detection.

By using subfragments of pJuC or p182 (Fig. 1C) and a cycloheximide block, IER6.3 and IER1.5 were mapped more accurately. Probes C2, C3, and N1-3 (Fig. 2B, lanes 2 to 6) detected IER6.3 with similar intensity, but only probes N2, N3, and C2 detected IER1.5 (the slight signal with probe N1 may be explained by a 10-nt sequence overlap), and probes N4 and N5 detected no IE transcripts. The major IE transcripts IER4.2 and IER2.9 and the 7-kb precursor were detected by control probes C1 (representing the right-hand end of U_L), C2, and C3 where appropriate (19) but not by probes N1 to N5. As mentioned above, the signal around 4 kb obtained with probes N2 and N3 may have been due to nonspecific cross-hybridization. As a second possibility, a computer search revealed two G+C-rich regions (30 nt in N2, 40 nt in N3) with 80% homology to IER4.2, which may account for some cross-hybridization. Together, these results suggest that IER6.3 traverses joined genome ends from about 0.96 to 0.01 m.u. and that IER1.5 is derived from IER6.3 by splicing, exon 1 being located within C2, representing the IER4.2-2.9 leader region, and exon 2 being located between the *NarI* and *SalI* sites of p182 (Fig. 1).

To map the 5' termini and splice site boundaries, we performed S1 nuclease protection and primer extension experiments. For Fig. 3A, p182 was cleaved at the unique *NotI* site, 5' end labeled with T4 polynucleotide kinase, and cleaved into two fragments with *HindIII*; the fragment shown in Fig. 1C (N6 with attached vector) was isolated and hybridized to RNA from BHV-1 K22-infected cells. After S1 nuclease digestion, a 5'-end-labeled fragment of 176 nt remained protected by BHV-1 RNA obtained under IE conditions (lane 1). An additional signal was observed at about 380 nt, with a series of weak bands below. Sequence

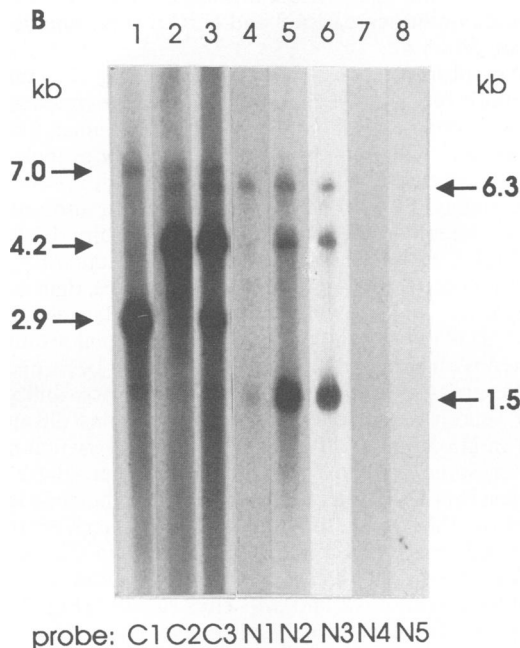
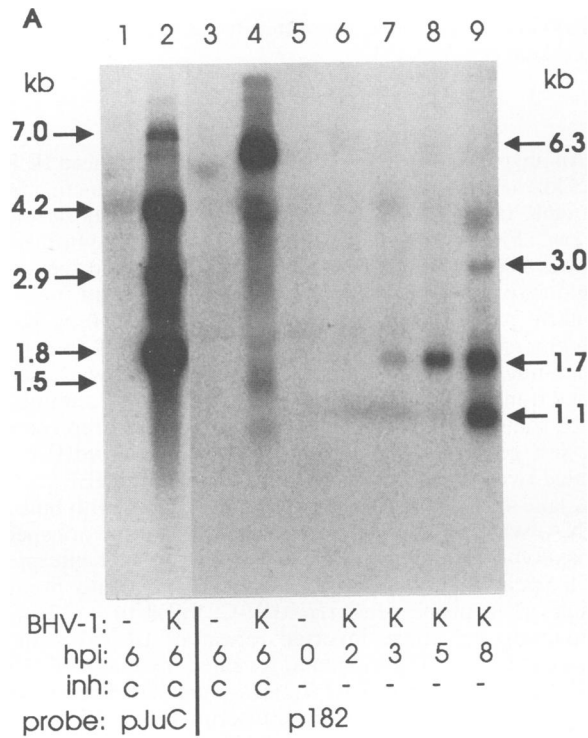


FIG. 2. Northern blot analysis of BHV-1 RNA using the probes described in Fig. 1C. (A) MDBK cells were mock infected (-) or infected with BHV-1 K22 (K). Total RNA was harvested at the indicated times (hours) p.i. (hpi) in the absence (-) or presence (c) of the inhibitor (inh) cycloheximide (100 µg/ml), separated by electrophoresis, blotted on nylon membranes, and hybridized with ³²P-labeled pJuC or p182, and transcripts were revealed by autoradiography. (B) Identical strips carrying blotted RNA isolated at 6 h p.i. from BHV-1 K22-infected, cycloheximide-treated cells were hybridized with probes C1 to C3 and N1 to N5 for fine mapping of transcripts. Calculated transcript sizes are indicated.

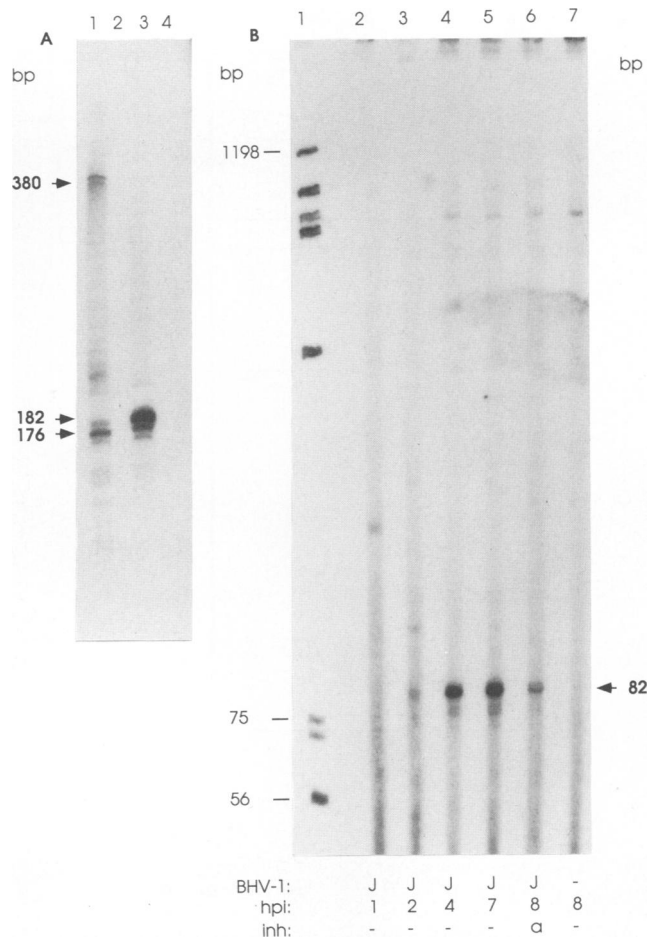


FIG. 3. S1 nuclease and primer extension analyses of IER1.5 and LR1.1. (A) Probe N6 (Fig. 1C) was 5' end labeled at the *NotI* site and hybridized to total RNA from mock-infected (lanes 2 and 4) or BHV-1 K22-infected (lanes 1 and 3) cells either treated with cycloheximide (lanes 1 and 2) or untreated and harvested at 8 h p.i. (lanes 3 and 4). Fragments protected from S1 nuclease digestion were analyzed on 6% polyacrylamide-urea gels. (B) For primer extension reactions, o22 (Fig. 1D) was 5' end labeled and hybridized to RNA from mock-infected (-) or BHV-1 strain Jura-infected (J) cells, either treated with the inhibitor (inh) cytosine arabinoside (a) or untreated (-), and harvested at the times (hours) p.i. (hpi) indicated. Reverse transcriptase from avian myeloblastosis virus was used to synthesize cDNA fragments, which were analyzed on an 8% polyacrylamide-urea sequencing gel. End-labeled *HinI* fragments of pGEM4 served as markers (lane 1).

analysis (see below) suggested that the 176-nt band represented hybridization to IER1.5 with protection up to the splice site and that the 380-nt band was due to hybridization to IER6.3 with protection ending within a sequence of short direct repeats (5). Misalignment in the repeat structures may have caused the full-length 648-nt probe to be S1 nuclease sensitive. With RNA obtained under late conditions (lane 3), the size of the principal protected fragment was clearly larger (approximately 182 nt) than the 176 nt observed under IE conditions but the 380-nt band was absent.

For Fig. 3B, we used 5'-end-labeled o22 (Fig. 1D) as the primer for reverse transcription and RNA from BHV-1 Jura-infected cells as the template. The resulting cDNA (approximately 82 nt) appeared with increasing intensity when RNA isolated at different times from 2 to 7 h p.i. was



FIG. 4. Nucleotide sequence of the BHV-1 (K22) genome segment specifying the IER4.2-2.9 leader RNA (A), which is also present in IER1.5; nucleotide sequence of the 5' genomic terminus (U_L) including the *circ* gene (B). Underlined portions: 1, TATA box; 2, transcription start site for the leader RNA; 3>, location of primer o10; <4, location of complementary probe o3; 5, splice donor site for IER1.5 (terminal GT of the intron); 6, octamer box; 7 and 8, first and last 14-nt direct repeats (repeated 14 times); 9, transcription start site for LR1.1; 10, splice acceptor site for IER1.5 (terminal AG of the intron); 11, *Nar*I site; 12, first ATG codon for *circ*; <13, location of complementary primer o22; 14, *Nor*I site; 15, TAG stop codon for *circ*; 16 and 18, polyadenylation signals for the *circ* and UL54 genes, respectively; 17, *Sall* site.

used; signal intensity was strongly reduced when entry into the late phase was blocked by inhibition of viral DNA synthesis with cytosine arabinoside. Therefore, this cDNA was derived from a late transcript, identified as LR1.1 by Northern blot analysis (data not shown) using subfragments N1 to N5, which located LR1.1 near the left genomic terminus, whereas ER1.7 and LR3.0 mapped further towards the right.

IER1.5 consists of the IER4.2-2.9 leader sequence spliced to the LR1.1 sequence just downstream from its 5' end. The transcription start site and the splice donor site of the leader RNA common to IER4.2 and IER2.9 have been mapped previously (19). The nucleotide sequence of the BHV-1 (K22) genome region specifying this leader RNA is displayed in Fig. 4A; the bases are numbered from 2456 to 2845 because they are part of an 8.1-kb sequence, to be published elsewhere (16), which includes the entire gene specifying IER4.2 and flanking regions. The same leader RNA also forms exon 1 of IER1.5, as will be shown below.

To analyze exon 2 of IER1.5, the left genomic terminus of BHV-1 was sequenced (Fig. 4B). The *Nor*I site used for S1 nuclease protection analysis (Fig. 3A) was located at nt 643 to 650, with nt 648 representing the 5'-end-labeled residue. By subtracting the 176-nt fragment protected under IE conditions (Fig. 3A, lane 1), nt 472 was identified as the last residue of the intron. The same splice junction was predicted from a consensus splice acceptor signal, with nt 471 to 472 forming the terminal AG of the intron. Thus, exon 2 of IER1.5 begins at nt 473.

In contrast, LR1.1 was not spliced but exhibited a 5' end located in the intron just upstream from the IER1.5 splice junction. This was concluded from the size of the 82-nt primer extension product (Fig. 3B), which positioned the transcription start site of LR1.1 at nt 466, measured from the 5' end of o22 (nt 547). Nearly the same result was obtained by S1 nuclease analysis; by subtracting the 182-nt fragment protected under late conditions (Fig. 3A, lane 3) from the

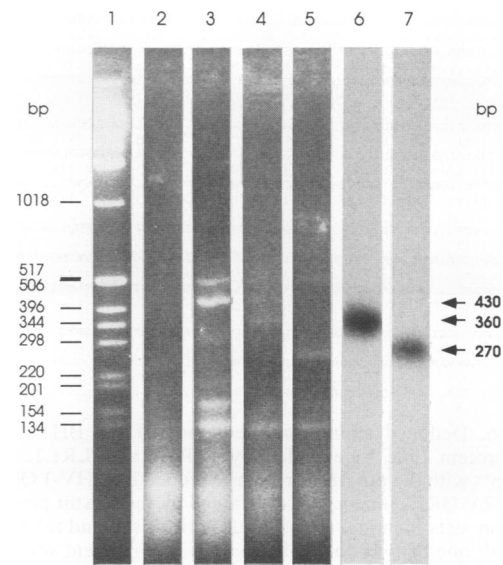


FIG. 5. PCR amplification of primer extension products. Unlabeled o22 was hybridized to RNA (5 µg) from mock-infected (lane 2) or BHV-1 K22-infected, cycloheximide-treated cells (lanes 3 to 7) and extended with reverse transcriptase; the products were amplified by using o22 and o10 as primers. Lanes: 1, size marker; 2 and 3, no cleavage; 4 and 5, cleavage of lane 3 products with *Kpn*I and *Nar*I or *Kpn*I, *Nhe*I, and *Nar*I, respectively; 6 and 7, Southern blot of lanes 4 and 5 probed with end-labeled o3.

size of the N6 probe, nt 467 was identified as the LR1.1 start site. Thus, transcription of LR1.1 starts 6 or 7 nt upstream of the IER1.5 splice junction. The three transcripts IER1.5, IER6.3, and LR1.1 share a common 3' terminus, because Northern blot analysis (Fig. 2B) defined as the boundary a *Sall* site located 0.9 kb downstream from the splice site and because a poly(A) addition signal occurs just 80 nt before the *Sall* site (Fig. 4B).

Northern blots suggested that the 5' terminus of IER6.3-1.5 coincides with the previously described 5' terminus of IER4.2-2.9 (19). However, extension of primer o22 (Fig. 3B) did not produce the expected 430-bp signal, although additional bands above the main band at 82 nt could be observed.

This problem was solved by using products of the o22 primer extension experiment for PCR with primers o22 and o10 and characterizing the products by restriction analysis (Fig. 5). Among several amplified PCR products (lane 3), only one band, at 430 bp, contained restriction sites which were consistent with the postulated structure of IER1.5; it was reduced to 360 bp when cut with *Kpn*I and *Nar*I (lane 4) and to 270 bp when cut with *Kpn*I, *Nhe*I, and *Nar*I (lane 5). Southern blot hybridization with o3 exclusively detected the 360-bp *Kpn*I-*Nar*I and 270-bp *Kpn*I-*Nhe*I fragments (lanes 6 and 7). The other bands neither exhibited the expected cleavage sites upstream from o22 nor hybridized with o3 and were therefore considered to be nonspecific PCR amplification products.

As final proof for transcription over the circularized genome, the 360-bp *Kpn*I-*Nar*I fragment was cloned and its nucleotide sequence was compared with sequences at both ends of the BHV-1 genome. The 360-bp sequence was perfectly colinear with the following three elements: it started with o10 (Fig. 4A; nt 2487 to 2510), continued with the leader sequence of IER4.2-2.9 until the regular 3' splice donor site (nt 2840), crossed over to the 5' splice acceptor

Reflecting this situation, the late rightward promoter constitutes a switch from IER1.5 to LR1.1, and both transcripts encode the same 247-residue *circ*-encoded protein.

The function of the *circ*-encoded protein remains unknown. Our finding that it arises under two widely different circumstances, at IE times from a circular template and at late times from an alternative promoter dependent on DNA synthesis, suggests a regulatory function connected with the BHV-1 genome structure. We therefore aim to isolate this protein and examine its role in circularization, inversion, cleavage, or packaging of BHV-1 genomes. The presence and similar location of a *circ* gene in VZV and EHV-1, with an equally unknown function, suggests that the novel features reported here for BHV-1 are worth looking for in other herpesviruses. The absence of *circ* from HSV-1 may signify that its function is not required for the HSV-1 genome, which continually exhibits joined termini owing to frequent inversion of both L and S components.

ACKNOWLEDGMENTS

We thank M. Ackermann, A. Bridgen, and A. Fiechter for critically reading the manuscript and A. Hug for photography.

This work was supported by grant 31-263346.89 from the Swiss National Science Foundation.

REFERENCES

1. Davison, A. J., and J. E. Scott. 1986. The complete DNA sequence of varicella-zoster virus. *J. Gen. Virol.* **67**:1759–1816.
2. Devereux, J., P. Haeblerli, and O. Smithies. 1984. A comprehensive set of sequence analysis programs for the VAX. *Nucleic Acids Res.* **12**:387–395.
3. Engels, M., C. Giuliani, P. Wild, T. M. Beck, E. Loepfe, and R. Wyler. 1986. The genome of bovine herpesvirus 1 (BHV-1) strains exhibiting a neuropathogenic potential compared to known BHV-1 strains by restriction site mapping and cross-hybridization. *Virus Res.* **6**:57–73.
4. Fraefel, C., B. Vogt, and M. Schwyzer. Unpublished data.
5. Hammerschmidt, W., H. Ludwig, and H.-J. Buhk. 1986. Short repeats cause heterogeneity at genomic terminus of bovine herpesvirus 1. *J. Virol.* **58**:43–49.
6. Hammerschmidt, W., H. Ludwig, and H.-J. Buhk. 1988. Specificity of cleavage in replicative-form DNA of bovine herpesvirus 1. *J. Virol.* **62**:1355–1363.
7. Harty, R. N., R. R. Yalamanchili, and D. J. O'Callaghan. 1991. Transcriptional analysis of the UL1 gene of equine herpesvirus 1: a gene conserved in the genome of defective interfering particles. *Virology* **183**:830–833.
8. Laux, G., A. Economou, and P. J. Farrell. 1989. The terminal protein gene 2 of Epstein-Barr virus is transcribed from a bidirectional latent promoter region. *J. Gen. Virol.* **70**:3079–3084.
9. Mellerick, D. M., and N. W. Fraser. 1987. Physical state of the latent herpes simplex virus genome in a mouse model system: evidence suggesting an episomal state. *Virology* **158**:265–275.
10. Misra, V., R. M. Blumenthal, and L. A. Babiuk. 1981. Proteins specified by bovine herpesvirus 1 (infectious bovine rhinotracheitis virus). *J. Virol.* **40**:367–378.
11. Poffenberger, K. L., and B. Roizman. 1985. A noninverting genome of a viable herpes simplex virus 1: presence of head-to-tail linkages in packaged genomes and requirements for circularization after infection. *J. Virol.* **53**:587–595.
12. Preston, C. M., and J. Russell. 1991. Retention of nonlinear viral DNA during herpes simplex virus latency in vitro. *Intervirology* **32**:69–75.
13. Rall, G. F., Z. Q. Lu, N. Sugg, R. A. Veach, and T. Ben Porat. 1991. Acquisition of an additional internal cleavage site differentially affects the ability of pseudorabies virus to multiply in different host cells. *J. Virol.* **65**:6604–6611.
14. Sanger, F., S. Nicklen, and A. R. Coulson. 1977. DNA sequencing with chain-terminating inhibitors. *Proc. Natl. Acad. Sci. USA* **74**:5463–5467.
15. Telford, E. A., M. S. Watson, K. E. McBride, and A. J. Davison. 1992. The DNA sequence of equine herpesvirus-1. *Virology* **189**:304–316.
16. Viček, C., O. Menekse, V. Pačes, and M. Schwyzer. Unpublished data.
17. Wirth, U. V., C. Fraefel, B. Vogt, C. Vlček, V. Pačes, and M. Schwyzer. 1992. Immediate-early RNA 2.9 and early RNA 2.6 of bovine herpesvirus 1 are 3' coterminal and encode a putative zinc finger transactivator protein. *J. Virol.* **66**:2763–2772.
18. Wirth, U. V., K. Gunkel, M. Engels, and M. Schwyzer. 1989. Spatial and temporal distribution of bovine herpesvirus 1 transcripts. *J. Virol.* **63**:4882–4889.
19. Wirth, U. V., B. Vogt, and M. Schwyzer. 1991. The three major immediate-early transcripts of bovine herpesvirus 1 arise from two divergent and spliced transcription units. *J. Virol.* **65**:195–205.
20. Wyler, R., M. Engels, and M. Schwyzer. 1989. Infectious bovine rhinotracheitis/vulvovaginitis (BHV-1), p. 1–72. *In* G. Wittmann (ed.), *Herpesvirus diseases of cattle, horses, and pigs. Developments in veterinary virology.* Kluwer Academic Publishers, Boston.
21. Yalamanchili, R. R., B. Raengsakulrach, R. P. Baumann, and D. J. O'Callaghan. 1990. Identification of the site of recombination in the generation of the genome of DI particles of equine herpesvirus type 1. *Virology* **175**:448–455.
22. Yalamanchili, R. R., B. Raengsakulrach, and D. J. O'Callaghan. 1990. Equine herpesvirus 1 sequence near the left terminus codes for two open reading frames. *Virus Res.* **18**:109–116.